
Efficient Generation of Diverse Cooperative Agents with World Models

Yi Loo, Akshunn Trivedi, Malika Meghjani

Singapore University of Technology and Design (SUTD)

yi_loo@mymail.sutd.edu.sg

{akshunn_trivedi, malika_meghjani}@sutd.edu.sg

Abstract

A major bottleneck in the training process for Zero-Shot Coordination (ZSC) agents is the generation of partner agents that are diverse in collaborative conventions. Current Cross-play Minimization (XPM) methods for population generation can be very computationally expensive and sample inefficient as the training objective requires sampling multiple types of trajectories. Each partner agent in the population is also trained from scratch, despite all of the partners in the population learning policies of the same coordination task. In this work, we propose that simulated trajectories from the dynamics model of an environment can drastically speed up the training process for XPM methods. We introduce XPM-WM, a framework for generating simulated trajectories for XPM via a learned World Model (WM). We show XPM with simulated trajectories removes the need to sample multiple trajectories. In addition, we show our proposed method can effectively generate partners with diverse conventions that match the performance of previous methods in terms of SP population training reward as well as training partners for ZSC agents. Our method is thus, significantly more sample efficient and scalable to a larger number of partners.

1 Introduction

An effective cooperative agent should generalize well to new partners and teammates in zero shot. However, this remains a challenging task for Reinforcement Learning (RL) agents, mainly due to the distributional shift of partner policies from training to those encountered in inference [3]. Recently, the Zero Shot Coordination (ZSC) problem [11] was proposed to test a cooperative agent’s ability to generalize to unseen partners not encountered during training. The most prominent way to train ZSC agents is through population-based training [20, 27, 37, 16, 36, 17, 22], where an ego agent is trained together with a population of diverse agents. Diverse agents also serve an additional purpose, which is to serve as holdout sets of novel partners to evaluate the performance of ZSC agents.

Thus, generating a diverse set of policies is a crucial step in the training and evaluation of many ZSC methods. However, generating diverse agents is very computationally expensive as each agent within the population is trained jointly [20, 37, 4] or sequentially [24] from scratch. Prominent diverse population generation methods uses cross-play minimization (XPM) [4, 24] which requires sampling additional trajectories in addition to the usual self-play trajectories during training. LIPO [4] for example requires sampling cross-play trajectories from every partner agent at every training step whereas CoMeDi [24] requires sampling mixed-play trajectories on top of self and cross-play trajectories at every training iteration to discourage agents from establishing handshakes during self-play training which causes self-sabotaging policies in cross-play. As a result, the amount of data required for training each agent scales up relative to the number of existing partner agents in the

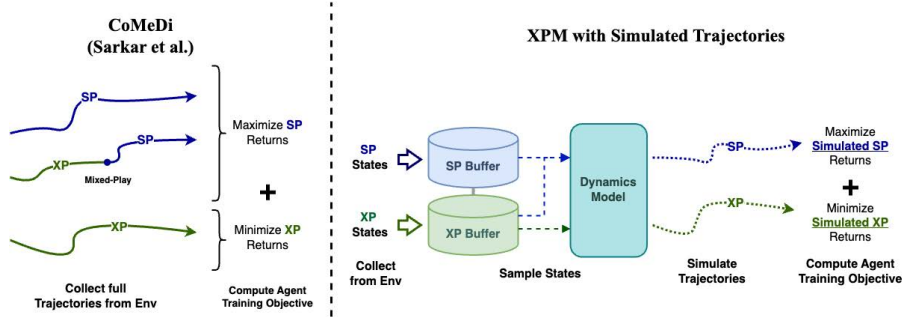


Figure 1: Diagram of the training process of XPM-Sim (right) compared to CoMeDi. Our key insight is that by expanding the starting states of SP simulated trajectories, we remove the need for Mixed Play trajectories while still producing policies that do not self-sabotage, resulting in a more sample efficient method.

population. Both methods also use on-policy methods [35] to train each agent within the population, which are known to be less sample efficient compared to off-policy or model-based methods [32].

In this work, we present a more efficient method for generating diverse cooperative agents. We focus our method on addressing two key areas of sample inefficiency of current XPM methods, that is the requirement to sample multiple types of trajectories and the lack of knowledge transfer between agents within the population as each agent is trained from scratch. At the same time, we also ensure that our method retains the ability to generate agents that are meaningfully diverse and do not self-sabotage. We propose that Model-Based Reinforcement Learning (MBRL) [34] could be useful for drastically improving the sample efficiency of XPM. In particular, we show that given an accurate dynamics model of the environment, we can derive a more efficient XPM objective by learning exclusively through simulated self and cross-play trajectories. In addition, we empirically also show that our proposed objective, XPM-Sim, removes the need for mixed-play trajectories while still producing agent policies that do not self-sabotage.

We then present XPM-WM, a more generalizable method for generating diverse agents with XPM-Sim via learned world models [6, 7]. Our method first trains a world model to act as a strong prior to bootstrap the training of individual partner agents. We then train diverse agents with simulated self and cross-play trajectories generated by the world model with XPM-Sim. We experimentally show on the popular Overcooked AI [3] environment that our proposed method XPM-WM is significantly more sample efficient when training individual XPM agents and also more scalable to greater number of agents within the population compared to previous XPM methods. Finally, we showcase the diversity of the generated agent population by training an ego agent with the population and evaluate it on a ZSC setting on both novel agent partners as well as real human partners.

To summarize, our contributions in this paper are as follows:

1. We introduce XPM-Sim, a sample efficient objective for generating diverse agents via XPM by training on simulated trajectories.
2. We empirically show that XPM-Sim removes the need for sampling mixed-play trajectories.
3. We propose XPM-WM, a generalizable method for XPM-Sim by utilizing world models to simulate self-play and cross-play trajectories.
4. We empirically show the gains in efficiency and scalability of XPM-WM on the Overcooked AI environment and that agents generated via XPM-WM are effective as training partners for ZSC agents.

2 Preliminaries

2.1 Zero-Shot Coordination (ZSC)

The Zero-shot Coordination (ZSC) problem is typically formulated as a Decentralized Markov Decision Process (Dec-MDP) or Decentralized (Partially Observable) MDPs for partially observable environments. The Dec-MDPs and Dec-POMDPs are represented by the tuple

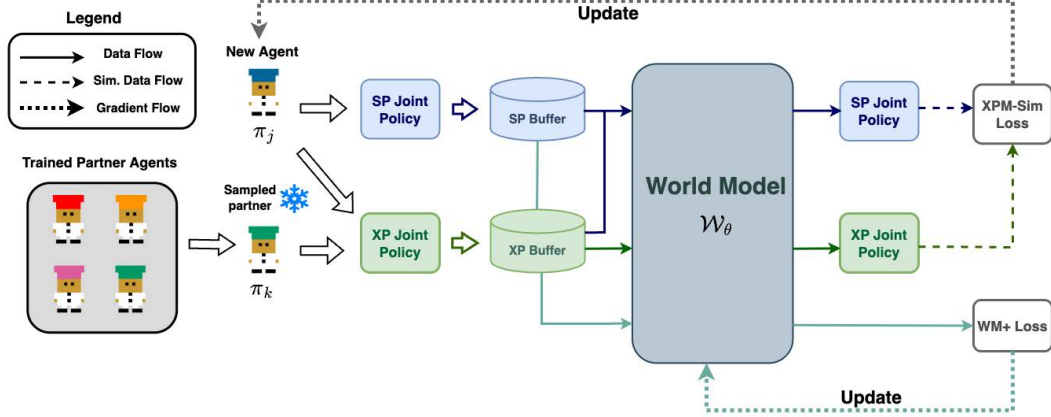


Figure 2: Diagram of the training process for XPM-WM. For the first phase, only the self-play (in blue) portion of the diagram is used and the agent is trained with just the objective SP. During the training of subsequent agents using XPM-Sim, the parameters of the partner agent is kept frozen while we continuously update the World Model.

$(\mathcal{S}, O, \{\mathcal{O}^i, \mathcal{A}^i\}_{i \in \mathcal{N}}, T, R, \gamma)$. \mathcal{S} represents the state space of the environment. \mathcal{N} represents the set of players in the environment, we focus on two-player tasks in this work hence in this case $\mathcal{N} = \{1, 2\}$. \mathcal{O}^i and \mathcal{A}^i are the observation and action spaces of the i -th player respectively. The observation function $O : \mathcal{S} \rightarrow \mathcal{O}^1 \times \mathcal{O}^2$ generates a player specific observation of the state. Note that even for fully observable Dec-MDP, different players can have different observations from a same state s due to player-specific indicators. We can write the joint action space as $\mathcal{A} : \mathcal{A}^1 \times \mathcal{A}^2$ and a joint action as $\mathbf{a} = (a^1, a^2)$. The transition function $T : \mathcal{S} \times \mathcal{A} \times \mathcal{S} \rightarrow [0, 1]$ represents the probability of reaching a subsequent state given a previous state and joint action. The reward function $R : \mathcal{S} \times \mathcal{A} \rightarrow \mathbb{R}$ gives a real valued reward after each state transition and finally γ represents the reward discount factor.

A joint policy $\pi : \pi^1 \times \pi^2$ acts on the Dec-MDP by producing (joint) action distributions, at every state $s \in \mathcal{S}$. Over a finite horizon H , the policy produces a joint trajectory, $\tau_\pi = (s_0, \mathbf{a}_0, \dots, s_{H-1}, \mathbf{a}_{H-1}, s_H)$, which can be further divided into player specific trajectories $\tau_\pi^i = (o_0^i, a_0^i, \dots, o_{H-1}^i, a_{H-1}^i, o_H^i)$. The discounted return for a trajectory is defined as $G(\tau) = \sum_{t=0}^{H-1} \gamma^t r(s_t, \mathbf{a}_t)$ and the expected return for a joint policy is defined as $J(\pi^1, \pi^2) = \mathbb{E}_{\tau \sim (\pi^1, \pi^2)}[G(\tau)]$. The self-play (SP) return, $J_{SP}(\pi_A)$ of policy π_A is when both players in the joint policy are identical copies, i.e. $\pi^1 = \pi^2 = \pi_A$. The cross-play (XP) return for two distinct policies, π_A and π_B , is then defined as: $J_{XP}(\pi_A, \pi_B) \equiv J(\pi_A, \pi_B) + J(\pi_B, \pi_A)$.

The objective of ZSC is then to produce an ego-agent, represented by policy π^e that can achieve high cross-play returns with policies drawn from unseen set of policies, Π_{test} . The ZSC objective is thus defined as $J_{ZSC}(\pi_e) = \max_{\pi^e} \mathbb{E}_{\pi^* \sim \Pi_{test}}[J_{XP}(\pi^e, \pi^*)]$. The original formulations of ZSC require the unseen policies, Π_{test} to be also trained using the same algorithm as π^e [11], but more recent works have expanded the formulation to include policies trained with other methods [19] or even human players [15, 30], which is more in-line with the formulation for Ad-hoc Teamplay as proposed by Stone et al. [26]. In this work we adopt the latter, broader definition of ZSC.

2.2 Diverse Population Generation with Cross-Play Minimization

We now formalize the problem of generating a diverse population of policies for a 2-player cooperative task. We are interested in generating a set of M agents each represented by policy π_j , $\mathcal{D} = \{\pi_1, \pi_2, \dots, \pi_m\}$ that are diverse in their behavioral conventions. A convention is defined as a joint policy $\pi_j = \pi_j^1 \times \pi_j^2$. Two policies, π_A and π_B are said to have compatible conventions if their joint cross-play objective is at least as high as the self-play objective [4]. Thus, a straightforward way to generate diverse policies is to ensure the pairwise cross-play objective for each distinct pairs of policies in the population is divergent from the individual policies' self-play objectives. This leads to a broad class of XPM methods, where the agents are trained to maximize J_{SP} while simultaneously minimizing the pairwise J_{XP} objective with respect to other agents in \mathcal{D} .

LIPO: LIPO proposed by Charakorn et al. [4] presents a straightforward method for XPM training. Specifically for given policy $\pi_j \in \mathcal{D}$, the LIPO method optimizes the following objective:

$$J_{LIPO}(\pi_j) = \max_{\pi_j} J_{SP}(\pi_j) - \lambda_{XP} \max_{\pi_k \in \mathcal{D} \setminus \pi_j} J_{XP}(\pi_j, \pi_k) \quad (1)$$

Although LIPO is effective in generating populations that have low cross-play returns, the choice to train all agents are updated concurrently could result in training instabilities. Furthermore, recent works [5, 24] demonstrated that naively doing cross-play minimization could result in policies that learn to perform handshakes and self-sabotage in cross-play.

CoMeDi: CoMeDi [24], was proposed as an augmentation on top of the LIPO objective to mitigate the issue of handshakes/self-sabotaging. Specifically, CoMeDi proposes adding a Mixed-Play (MP) term to the overall training objective. A MP trajectory is generated by starting with a cross-play partner from \mathcal{D} and at a random timestep, t^* before horizon H , switches to self-play partner. The trajectory before t^* is discarded and the remaining trajectory segment is trained with the self-play objective. The full CoMeDi objective then becomes

$$J_{CoMeDi}(\pi_j) = \max_{\pi_j} (J_{SP}(\pi_j) + \lambda_{MP} J_{MP}(\pi_j)) - \lambda_{XP} \max_{\pi_k \in \mathcal{D} \setminus \pi_j} J_{XP}(\pi_j, \pi_k). \quad (2)$$

Additionally, CoMeDi also proposed to train each agent sequentially rather than concurrently, where agents are trained one at a time while keeping previous agent’s policies frozen, resulting in a more stable training process.

2.3 Limitations of Cross-Play Minimization

We identify that current XPM methods are sample inefficient in two key areas: (a) the need to sample additional XP trajectories from each previous partner at every training iteration. This is to compute the XP objective but also to determine the maximum XP partner. (b) The need to sample MP trajectories to mitigate self-sabotage and (c) the lack of knowledge transfer between agents in \mathcal{D} during training. In the following sections, we outline our proposed framework of using Model-Based Reinforcement Learning (MBRL) approach to address these limitations. We first demonstrate how simulated trajectories from a dynamics model can increase the sample efficiency of XPM. We then outline our proposed approach, XPM-WM as a more generalizable method where simulated trajectories are generated via a learned World Model (WM). We also show that utilizing WMs in XPM also amortizes the cost of training subsequent agents by providing a strong prior to bootstrap the training process of subsequent agents.

3 Cross-Play Minimization with Simulated Trajectories

For a given Dec-MDP, if the forward dynamics $T(s, \mathbf{a})$ and $R(s, \mathbf{a}, s')$ are known, or accurately estimated via a model F , we can generate a simulated trajectory from any state $s \in \mathcal{S}$. Specifically, we define $\hat{\tau}_F^\pi(s) = (s, \mathbf{a}_0, \hat{s}_1, \mathbf{a}_1, \dots, \hat{s}_{H'-1}, \mathbf{a}_{H'-1}, \hat{s}_{H'})$ as a simulated trajectory with simulation horizon H' that is generated using model F starting from state s with joint policy π , where \hat{s}_t is a simulated state at time t . Given two distinct policies, π_j and π_k in \mathcal{D} , we can generate SP and XP simulated trajectories, $\hat{\tau}^{SP} = \hat{\tau}_F^{(\pi_j, \pi_j)}(s)$ and $\hat{\tau}^{XP} = \hat{\tau}_F^{(\pi_j, \pi_k)}(s)$. We are then able train a (joint) policy over simulated trajectories by maximizing the expected simulated returns, $\hat{J}(\pi) = \mathbb{E}_{\hat{\tau}_F \sim (\pi), s \in \mathcal{S}} [G(\hat{\tau}_F(s))]$. Note that the current objective allows trajectories to be simulated from any starting state in \mathcal{S} . However, for XPM training we restrict the set of starting states of simulated SP and XP to the set of *reachable* states which we define in below:

Definition 3.1. For a two-player Dec-MDP given a joint policy $\pi = (\pi^1, \pi^2)$ the set of reachable states, $\mathcal{S}^\pi \subseteq \mathcal{S}$ consist of any *reachable* state under joint policy π from starting state $s_0 \sim p(s_0)$ within horizon H .

For each policy in \mathcal{D} , we can also define the reachable self-play states, $\mathcal{S}_{SP}^j = \mathcal{S}^{\pi_j}$ and reachable cross-play states, $\mathcal{S}_{XP}^{j,k} = \mathcal{S}^{(\pi_j, \pi_k)}$. This then allows us to define $\widehat{J}_{SP}(\pi^j)$ and $\widehat{J}_{XP}(\pi^j, \pi^k)$ and arrive at a similar XPM objective as in Equation 1. However, without the addition of Mixed-Play objective, policies may still establish handshakes and learn to self-sabotage. We propose that we are able to remove the need of Mixed play objective by simply expanding the starting states of simulated SP trajectories to include reachable XP states.

Proposition 3.2. *Simulated SP trajectories, $\hat{\tau}_F^{\pi_{SP}}(s_{xp})$ generated via dynamics model F from any cross-play state, $s_{xp} \in \mathcal{S}_{XP}$ is equivalent to generating Mixed-Play trajectory in terms of mitigating handshake and self-sabotage behavior.*

We provide a proof of Proposition 3.2 in Appendix A. We then experimentally show this to be true in the following subsection. We can now construct a XPM training objective with simulated trajectories, XPM-Sim:

$$\begin{aligned} J_{XPMSim}(\pi_j) &= \max_{\pi_j} \widehat{J}_{SP}(\pi_j) - \lambda_{XP} \max_{\pi_k \in \mathcal{D} \setminus \pi_j} \widehat{J}_{XP}(\pi_j, \pi_k), \\ \text{where } \widehat{J}_{SP}(\pi_j) &= \mathbb{E}_{\hat{\tau}_F \sim (\pi_j), s \in \{\mathcal{S}_{SP}^j, \mathcal{S}_{XP}^{j,l}\}} [G(\hat{\tau}_F(s))], \quad \pi_l \in \mathcal{D} \setminus \pi_j, \\ \text{and } \widehat{J}_{XP}(\pi_j, \pi_k) &= \mathbb{E}_{\hat{\tau}_F \sim (\pi_j, \pi_k), s \in \mathcal{S}_{XP}^{j,k}} [G(\hat{\tau}_F(s))]. \end{aligned} \quad (3)$$

Note the above formulation allows from simulated SP trajectories to start from reachable SP states and reachable XP states with *any* agent in \mathcal{D} and not just the maximum XP partner. XPM-Sim provides a significantly more sample efficient training process over CoMeDi as (i) XPM-Sim does not require sampling Mixed-Play trajectories from the environment at every training iteration, (ii) even though SP and XP trajectories are required, they can be reused by storing them in SP and XP replay buffers and (iii) the maximum XP partner can be determined by looking at the latest trajectories in the replay buffer rather than resampling at every iteration. We show an outline of XPM-Sim in Figure 1 and contrast it with CoMeDi.

3.1 Empirical Analysis of Self-Sabotage Behavior

We will now empirically show Proposition 3.2 to be true via a simple toy experiment. We specifically want to compare the amount of self-sabotaging behavior in agents trained using XPM-Sim with other XPM methods, LIPO and CoMeDi. As it is challenging to define what constitutes self-sabotaging behavior in more complex cooperative environments, we conduct this experiment in the simple Multi Particle Environment (MPE) [18]. Specifically, we adopt the Multi Particle Point Mass Rendezvous (MPPMR) task proposed by [4], where agents, represented as point particles are tasked to rendezvous at any of the four evenly spaced checkpoints in the environment.

To adapt this task for checking self-sabotage behavior, we add a fixed boundary to the environment. Any agent particle that leaves the boundary of the environment will result in the episode to prematurely terminate. Hence, an agent that has learned to self-sabotage in cross-play can simply immediately go out of environment boundary and thus minimize the cross-play returns without learning to be meaningfully incompatible in terms of conventions with its partner agent.

As the forward dynamics of the MPE environment are determined by series linear dynamical equations, we can deterministically compute the forward dynamics of the MPPMR task from all starting states, which in turn allows us to simulate self and cross-play trajectories for XPM-Sim. We train a total of $M = 8$ agents for each method and look at the number of instances where each agent in the population exhibits self-sabotaging behavior, which we determine by the fraction of early terminations in cross-play.

Results: We present the results in Table 1. Our results show XPM-Sim exhibits significantly less self-sabotage behavior than LIPO. More notably, XPM-Sim also exhibits less self-sabotage behavior as compared to CoMeDi. This suggests that XPM-Sim is more effective at mitigating self-sabotage behavior as XPM-Sim simulates new trajectories from every real cross and self-play states. This essentially allows the agent to simulate mixed-play from every state of cross-play trajectories, whereas in CoMeDi mixed-play trajectories only utilizes one arbitrary start state per cross-play trajectory while discarding every preceding state. Finally we also show that XPM-Sim achieves comparable self-play rewards as compared to CoMeDi and LIPO.

4 XPM-WM: Cross-Play Minimization with World Models

Although XPM-Sim is a more efficient for generating diverse agents, the requirement for the full dynamics model, F to be known could be impractical for more complex cooperative environments and tasks. In cases where the F is not easily obtainable, we propose to instead estimate F using a learned World Model [6].

Table 1: Results of the MPPMR environment. The first 8 columns indicate the proportion of self-sabotage behaviors when in Cross-Play with preceding agents. E.g. Agent 4 will be paired with agents 1,2, and 3, with 1.0 indicating every episode containing self-sabotage behavior with 0 indicating None. SP indicates the average SP rewards across all 8 agents and XP indicates the average cross-play rewards.

	1	2	3	4	5	6	7	8	Average	SP \uparrow	XP \downarrow
LIPO	0.0	1.0	1.0	0.33	0.5	0.25	0.98	0.65	0.59	2.12	-130.65
CoMeDi	0.0	0.0	0.0	0.0	0.0	0.0	0.175	0.57	0.09	30.67	-114.01
XPM-Sim (Ours)	0.0	0.0	0.0	0.0	0.0	0.0	0.09	0.0	0.011	21.50	-114.50

We introduce XPM-WM, a method for generating diverse agents with XPM with simulated trajectories generated via a learned world model. XPM-WM consist of two training phases, the first phase involves learning a world model \mathcal{W}_θ , parameterized by θ together with an initial SP agent π_0 . The trained world model is then used to bootstrap the training process of subsequent M agents in \mathcal{D} using the XPM-Sim training objective outlined in Equation 3. On top of the increase in sample efficiency provided by XPM-Sim, using a World Model also makes the XPM training process more efficient by providing a strong prior in form of learned state representation from \mathcal{W}_θ , effectively transferring knowledge about the environment across agents, rather than training each of them from scratch.

We will now describe in detail the training process for XPM-WM. We first describe how we adapt the Dreamer [8] world models to a two player cooperative task and self-play training. We then describe the training process for the world model. Finally, we describe how we train agents using XPM-Sim with the learned model. We show an overview of XPM-WM in Figure 2.

4.1 World Models for Self-Play Training

We use the Dreamer (v3) [8, 9] architecture as the base of the world model and make changes to adapt it for self-play training. We inherit the Recurrent State Space Model (RSSM) which includes the encoder, recurrent state model, decoder, reward predictor, and continue predictor heads:

$$\begin{aligned}
&\text{Recurrent state model: } h_t = f_\theta(h_{t-1}, z_{t-1}, a_{t-1}^1, a_{t-1}^2) & \text{Transition predictor: } \hat{z}_t \sim p_\theta(\hat{z}_t | h_t) \\
&\text{Encoder: } z_t \sim q_\theta(z_t | h_t, o_t^1, o_t^2) & \text{Reward predictor: } \hat{r}_t \sim p_\theta(\hat{r}_t | h_t, z_t) \\
&\text{Decoder: } \hat{o}_t^i \sim p_\theta(\hat{o}_t^i | h_t, z_t^i), i \in \{1, 2\} & \text{Continue predictor: } \hat{\gamma}_t \sim p_\theta(\hat{\gamma}_t | h_t, z_t).
\end{aligned} \tag{4}$$

To facilitate a two-player setup, the RSSM now takes the previous joint actions of both players, a_{t-1}^1 and a_{t-1}^2 . Similarly, the encoder model also takes the joint observations o_t^1 and o_t^2 and outputs a distribution of the latent representation of the current state.

Player-specific Latent Representation: We modify the decoder model to reconstruct player specific observations from the player-specific state representation z_t^i . To obtain $z_t^i = (z_t^{joint}, z_t^{p_i})$, we first partition the state representation z_t into parts, which consists a joint representation, z_t^{joint} and two player-centric representations, $z_t^{p_i}$. z_t^{joint} represents global information in the state that are visible to all players (i.e. positions of certain objects) whereas $z_t^{p_i}$ represents player-specific information about the state (i.e. current position of the player). In practice we partition z_t into z_t^{joint} and by the number of discrete distributions. Specifically, out of the N discrete distributions in z_t , we set the first $K < N$ distributions as z_t^{joint} and the remaining $(N - K)$ distributions are equally divided into $z_t^{p_i}$, and each $z_t^{p_i}$ would then consist of $\frac{(N-K)}{2}$ distributions.

Event-based Rewards: We also modify the reward predictor to predict event-based rewards [36] over scalar rewards. Specifically, the reward predictor predicts a vector, where each column is a binary value indicating if an event or sub-task within the environment has been executed by a player i in the current state t . In practice, we model the reward predictor as a r -dimensional Bernoulli distribution, where r is the product of the number events and the number of players. For learning the policy in simulation, we compute the scalar reward as a linear function of the predicted event vector with a constant weight w^r . We find that this change greatly helps the World Model to effectively learn the transitional dynamics of the 2-player cooperative environment as it serves as a form of inductive bias that allow the model to tie player specific actions to the latent representation. We provide more details of the events specific to the environments we used in Appendix D.2.

World Model Loss: We use the Dreamer objective to train all the components in the World Model, which consists of the reconstruction, reward and continue predictor log loss, together with the KL Divergence term between $q_\theta(z_t)$ and $p_\theta(\hat{z}_t)$ [8].

$$\mathcal{L}_\theta = \mathbb{E}_{q_\theta} \left[\sum_{t=1}^H \left[\sum_{i=1}^2 -\ln p_\theta(o_t^i | h_t, z_t^i) \right] - \ln p_\theta(\mathbf{r}_t | h_t, z_t) - \ln p_\theta(\gamma_t | h_t, z_t) \right. \\ \left. + \beta KL[q_\theta(z_t | h_t, \mathbf{o}_t) || p_\theta(\hat{z}_t | h_t)] \right] \quad (5)$$

Finally, we also employ KL balancing [8] and free nats [9] for the KL loss term as introduced in later versions of the Dreamer model.

Actor and Critic: The actor takes in the player specific latent representation \hat{z}_t^i and outputs the player action distribution. The joint actions are then fed back to the RSSM to simulate future parts of the trajectory. For the Critic, we employ the Centralized Training and Decentralized (CTDE)[14, 23] approach popular in MARL methods and train a centralized critic for each agent pair. The centralized critic take the full state representation \hat{z}_t as input and outputs a distribution estimating the returns of simulated trajectories. Specifically for each agent j in \mathcal{D} , we have:

$$\text{Actor:} \quad a_t^i \sim \pi_{\phi^1}(a_t^i | \hat{z}_t^i), i \in \{1, 2\} \quad \text{Centralized Critic:} \quad v_{\psi_j^j}(\hat{z}_t) \approx G(\hat{\tau}_{\mathcal{W}_\theta}(s_t)). \quad (6)$$

Where ϕ^j are parameters of the actor, ψ_j^j the parameters of the centralized SP critic and ψ_k^j are parameters for the centralized XP critic for joint policy (π_j, π_k) . For an agent population of size M we train a total of $\frac{M(M+1)}{2}$ critics as we train each agent sequentially.

4.2 Training Subsequent Agents with a Learned World Model

For the second phase XPM-WM’s training process, we train each subsequent agent in \mathcal{D} sequentially using the XPM-Sim objective. We also continue fine-tuning the learned World Model, \mathcal{W}_θ with real cross and self-play trajectories. As in XPM-Sim, we maintain a separate SP and XP replay buffer and sample real trajectories to the update the World Model. As the actor parameters of the previous agents are fixed, we would want to update the World Model such that its latent distribution does not drift too far away from that of proceeding agents, especially for the set of XP reachable states $\mathcal{S}_{\mathcal{XP}}$. This is so that proceeding agents will produce consistent actions to generate XP trajectories. Hence we add an additional KL Divergence to the world model training loss,

$$\mathcal{L}_{\theta^j}^{WM+} = \mathcal{L}_{\theta^j}^{WM} + \gamma KL[q_{\theta^j}(z_t | h_t, \mathbf{o}_t) || q_{\theta^k}(z_t | h_t, \mathbf{o}_t)], \mathbf{o}_t \sim (\pi_j, \pi_k) \quad (7)$$

where \mathcal{L}^{WM} is world model loss as in Equation 5, θ^j are the parameters of the world model during the training process of agent j and θ^k the (fixed) parameters of the world model during the training process of preceding agent k . After the training for agent j is complete, we add WM \mathcal{W}_{θ^j} and policy π_j to the pool of partner agents.

5 Experiments

In this section we provide experimental evaluation of XPM-WM. In Section 5.1 we show the efficiency gains of XPM-WM compared to other XPM methods. In Section 5.2, we evaluate the diversity of the agents generated via XPM-WM on a full ZSC setting on holdout set of partners. In Section 5.3 we extend the ZSC setting to real human partners and finally in Section 5.4, we conduct a qualitative analysis on how well the diverse population covers different conventions present in human partners. We also include more detailed results in the Appendix as well as additional ablation studies of the effects of the vectorized reward and the dynamics model on the training efficiency.

Environment: We evaluate XPM-WM on the popular Overcooked AI cooperative environment [3]. Two players control two separate cooks in the environment and are tasked to deliver as many soups as possible in a given time frame. To be successful, agents have to subdivide tasks among themselves, ensure that they do not impede their partner’s progress and help them where necessary. We conduct our experiments on the five baseline layouts in Overcooked AI.

Baselines: We compare XPM-WM with two other cross-play minimization approaches, LIPO [4] and CoMeDi [24] which we described in detail in Section 2.2. Both methods are implemented using MAPPO [35]. ADVERSITY [5] is another prominent cross-play minimization method. However, we omit it as a baseline comparison since it is designed to model beliefs in partially observable environments whereas our method mainly focuses on fully observable games.

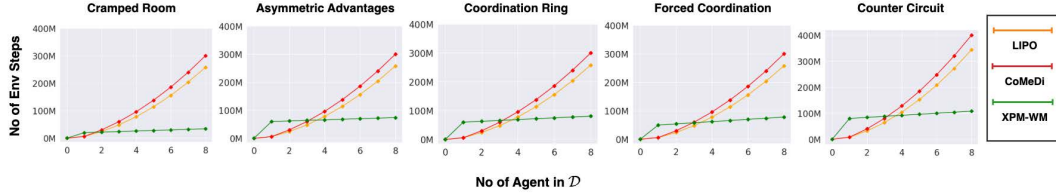


Figure 3: Scaling by number of agents. We show the training cost in terms of environmental steps for all 5 Overcooked layouts as number agents M in the population increases. LIPO and CoMeDi both have compounding increases in environmental steps required as M increases due to the requirement to sample additional trajectories whereas XPM-WM has more linear increase by first training an expensive World Model which compensates the cost of training subsequent agents.

5.1 Sample Efficiency Comparisons

Similar to the MPPMR environment, we train $M = 8$ agents for all three methods across all five layouts for a total of 40 agents per layout. We plot the **total number of environment steps** for each method against the number of agents in \mathcal{D} for all 5 Overcooked base layouts. We include self, cross and mixed play trajectories required for each method and show the plot in Figure 3.

Results: We show that though training the initial agent with World Model incurs a higher training cost than normal SP, the framework of using a pre-trained world model results in an overall more sample efficient method as the number of agents, M increases, with all layouts at least 3 times more sample efficient as compared to CoMeDi when scaled to 8 agents. This is primarily due to the significantly reduced training steps needed for subsequent agents due to the bootstrapping of the pre-trained World Model (we show the comparison in terms training steps for a single agent in Appendix H.1. Furthermore, the use of simulated trajectories also amortizes the cost of sampling additional XP and MP trajectories.

5.2 Ego Agent Training

We train an ego agent with the agent population generated using LIPO, CoMeDi and XPM-WM. We use HiPT [16] as the ego agents. We then train separate holdout population from all the methods to validate the ego-agents’s generalizability to novel partners. We present the average pair-wise rewards (Ego agent with hold-out populations) across all 5 Overcooked layouts in Table 2 and provide layout specific results in Appendix H.3.

Table 2: Results for Ego agents averaged across 5 Overcooked layouts . For each entry we compute the mean number dishes served as well as the standard error over 40 XP episodes for each partner agent in holdout population.

	E-LIPO	E-CoMeDi	E-XPM-WM (Ours)
LIPO	5.68 ± 3.27	5.32 ± 3.53	4.55 ± 3.32
CoMeDi	6.23 ± 3.02	6.01 ± 3.82	6.36 ± 3.11
XPM-WM (Ours)	4.68 ± 3.62	3.51 ± 3.56	6.51 ± 4.04
Average	5.59 ± 3.31	4.94 ± 3.64	5.80 ± 3.45

Results: Our results show the ego agent trained with XPM-WM achieved the highest average score across the 3 different holdout populations as compared to LIPO and CoMeDi. For the individual, WPM-XP also achieves comparable results to the other two baselines (differing no more than 3 average dishes from best performing agent). This suggests that the population generated by XPM-WM is comparable in diversity as the other baseline XPM methods while being significantly more sample efficient.

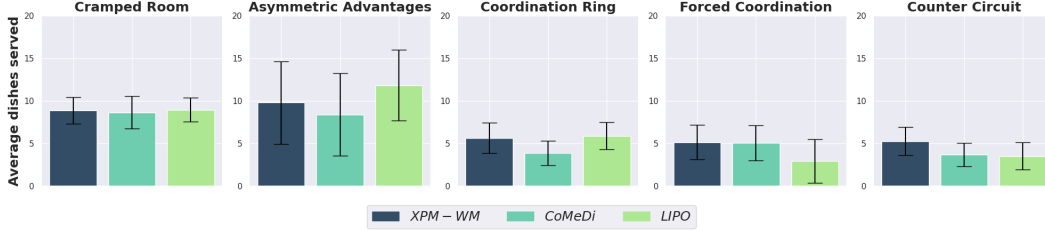


Figure 4: A comparison of the user study scores for HiPT ego agent trained with XPM-WM, CoMeDi and LIPO. Error bars represent the standard error.

5.3 User Studies

We then conduct an IRB approved user study by pairing the 3 ego agents used in Section 5.2 with 40 real human partners. Each human partner plays a total of 20 games with randomized layout and partners. We compare the average scores of each of the 3 ego agents when partnered with human partners and visualize the results in Figure 4.

Results: We find that the ego agents trained with population generated via XPM-WM achieves similar scores as compared to other ego agents, which suggest a comparable population diversity of XPM-WM as compared to other baselines. We have also found the results in the user studies to be consistent with the results on the hold out partner population.

5.4 Diversity Analysis

We then conduct further qualitative analysis on whether the ego agents can adapt to the diverse conventions present in the human partners. To do so, we isolate three common behaviors: plating frequency, onion picking frequency, and amount of movement in the environment. We then determine if a human partner has a high or low preference towards the behavior if their frequency/amount of said behavior is half standard deviation away from the mean of all humans for that agent. We then compute the average score for partners of said convention and show how much it deviates from the score with all human conventions. We show this comparison in Table 3. Overall our analysis shows that the ego agent trained with the XPM-WM generated population exhibits the least amount of deviation across all 6 conventions as compared to the other two baselines, suggesting the population is sufficiently diverse to cover a variety of human behavioral preferences.

Table 3: Comparison of difference in average number of dishes served with specific human conventions relative to all humans across all Overcooked environments.

	Plating Preference		Onion Picking Preference		Movement Activity Preference	
	High	Low	High	Low	High	Low
E-XPM-WM (Ours)	0.74	-0.43	1.3	-1.33	0.17	-0.20
E-LIPO	1.76	-1.17	1.14	-0.4	1.13	-0.51
E-CoMeDi	1.72	-1.87	0.90	-0.44	0.30	-0.59

6 Conclusion

In this work, we introduced XPM-WM, an efficient method for generating diverse agents for Zero-Shot Coordination. Our method is able to train agents with cross-play minimization in a more efficient manner by first learning a World Model and learning via simulated trajectories. We show that our method is significantly more sample efficient compared to the current XPM methods when training individual agents while achieving the same level of performance in terms population diversity. We also show our method is more scalable as compared to the other methods when the number of agents increase. For future work, we hope to extend our approach of using World Models for methods beyond cross-play minimization. We also hope to directly apply MBRL methods such as World Models on the training of the ego agent itself.

Acknowledgments and Disclosure of Funding

This project is jointly supported by the National Research Foundation Singapore and DSO National Laboratories under the AI Singapore Programme (Award Number: AISG2-RP-2020-016) and the Google South & South East Asia Research Award (2024).

References

- [1] A. Bar, G. Zhou, D. Tran, T. Darrell, and Y. LeCun. Navigation world models. *arXiv preprint arXiv:2412.03572*, 2024.
- [2] J. Bruce, M. D. Dennis, A. Edwards, J. Parker-Holder, Y. Shi, E. Hughes, M. Lai, A. Mavalankar, R. Steigerwald, C. Apps, et al. Genie: Generative interactive environments. In *Forty-first International Conference on Machine Learning*, 2024.
- [3] M. Carroll, R. Shah, M. K. Ho, T. Griffiths, S. Seshia, P. Abbeel, and A. Dragan. On the utility of learning about humans for human-ai coordination. *Advances in neural information processing systems*, 32, 2019.
- [4] R. Charakorn, P. Manoonpong, and N. Dilokthanakul. Generating diverse cooperative agents by learning incompatible policies. In *The Eleventh International Conference on Learning Representations*, 2023.
- [5] B. Cui, A. Lupu, S. Sokota, H. Hu, D. J. Wu, and J. N. Foerster. Adversarial diversity in hanabi. In *The Eleventh International Conference on Learning Representations*, 2023.
- [6] D. Ha and J. Schmidhuber. World models. *arXiv preprint arXiv:1803.10122*, 2018.
- [7] D. Hafner, T. Lillicrap, J. Ba, and M. Norouzi. Dream to control: Learning behaviors by latent imagination. In *International Conference on Learning Representations*, 2020.
- [8] D. Hafner, T. P. Lillicrap, M. Norouzi, and J. Ba. Mastering atari with discrete world models. In *International Conference on Learning Representations*, 2021.
- [9] D. Hafner, J. Pasukonis, J. Ba, and T. Lillicrap. Mastering diverse domains through world models. *arXiv preprint arXiv:2301.04104*, 2023.
- [10] A. Hu, L. Russell, H. Yeo, Z. Murez, G. Fedoseev, A. Kendall, J. Shotton, and G. Corrado. Gaia-1: A generative world model for autonomous driving. *arXiv preprint arXiv:2309.17080*, 2023.
- [11] H. Hu, A. Lerer, A. Peysakhovich, and J. Foerster. “other-play” for zero-shot coordination. In *International Conference on Machine Learning*, pages 4399–4410. PMLR, 2020.
- [12] H. Hu, A. Lerer, B. Cui, L. Pineda, N. Brown, and J. Foerster. Off-belief learning. In *International Conference on Machine Learning*, pages 4369–4379. PMLR, 2021.
- [13] D. P. Kingma, M. Welling, et al. Auto-encoding variational bayes, 2013.
- [14] L. Kraemer and B. Banerjee. Multi-agent reinforcement learning as a rehearsal for decentralized planning. *Neurocomputing*, 190:82–94, 2016.
- [15] Y. Li, S. Zhang, J. Sun, W. Zhang, Y. Du, Y. Wen, X. Wang, and W. Pan. Tackling cooperative incompatibility for zero-shot human-ai coordination. *Journal of Artificial Intelligence Research*, 80:1139–1185, 2024.
- [16] Y. Loo, C. Gong, and M. Meghiani. A hierarchical approach to population training for human-ai collaboration. In *Proceedings of the Thirty-Second International Joint Conference on Artificial Intelligence*, pages 3011–3019, 2023.
- [17] X. Lou, J. Guo, J. Zhang, J. Wang, K. Huang, and Y. Du. Pecan: Leveraging policy ensemble for context-aware zero-shot human-ai coordination. In *Proceedings of the 2023 International Conference on Autonomous Agents and Multiagent Systems*, pages 679–688, 2023.

- [18] R. Lowe, Y. Wu, A. Tamar, J. Harb, P. Abbeel, and I. Mordatch. Multi-agent actor-critic for mixed cooperative-competitive environments. *Neural Information Processing Systems*, 2017.
- [19] K. Lucas and R. E. Allen. Any-play: An intrinsic augmentation for zero-shot coordination. In *Proceedings of the 21st International Conference on Autonomous Agents and Multiagent Systems*, pages 853–861, 2022.
- [20] A. Lupu, B. Cui, H. Hu, and J. Foerster. Trajectory diversity for zero-shot coordination. In *International Conference on Machine Learning*, pages 7204–7213. PMLR, 2021.
- [21] S. Prasanna, K. Farid, R. Rajan, and A. Biedenkapp. Dreaming of many worlds: Learning contextual world models aids zero-shot generalization. *Reinforcement Learning Journal*, 1, 2024.
- [22] M. Rahman, J. Cui, and P. Stone. Minimum coverage sets for training robust ad hoc teamwork agents. In *Proceedings of the AAAI Conference on Artificial Intelligence*, volume 38, pages 17523–17530, 2024.
- [23] T. Rashid, M. Samvelyan, C. S. De Witt, G. Farquhar, J. Foerster, and S. Whiteson. Monotonic value function factorisation for deep multi-agent reinforcement learning. *Journal of Machine Learning Research*, 21(178):1–51, 2020.
- [24] B. Sarkar, A. Shih, and D. Sadigh. Diverse conventions for human-ai collaboration. *Advances in Neural Information Processing Systems*, 36:23115–23139, 2023.
- [25] J. Schulman, P. Moritz, S. Levine, M. Jordan, and P. Abbeel. High-dimensional continuous control using generalized advantage estimation. *arXiv preprint arXiv:1506.02438*, 2015.
- [26] P. Stone, G. Kaminka, S. Kraus, and J. Rosenschein. Ad hoc autonomous agent teams: Collaboration without pre-coordination. In *Proceedings of the AAAI Conference on Artificial Intelligence*, volume 24, pages 1504–1509, 2010.
- [27] D. Strouse, K. McKee, M. Botvinick, E. Hughes, and R. Everett. Collaborating with humans without human data. *Advances in Neural Information Processing Systems*, 34:14502–14515, 2021.
- [28] D. Valevski, Y. Leviathan, M. Arar, and S. Fruchter. Diffusion models are real-time game engines, 2024. URL <https://arxiv.org/abs/2408.14837>.
- [29] A. Venugopal, S. Milani, F. Fang, and B. Ravindran. Mabl: Bi-level latent-variable world model for sample-efficient multi-agent reinforcement learning. In *Proceedings of the 23rd International Conference on Autonomous Agents and Multiagent Systems*, pages 1865–1873, 2024.
- [30] X. Wang, S. Zhang, W. Zhang, W. Dong, J. Chen, Y. Wen, and W. Zhang. Zsc-eval: An evaluation toolkit and benchmark for multi-agent zero-shot coordination. *Advances in Neural Information Processing Systems*, 37:47344–47377, 2024.
- [31] X. Wang, Z. Zhu, G. Huang, X. Chen, J. Zhu, and J. Lu. Drivedreamer: Towards real-world-drive world models for autonomous driving. In *European Conference on Computer Vision*, pages 55–72. Springer, 2024.
- [32] L. Weng. Policy gradient algorithms. *lilianweng.github.io*, 2018. URL <https://lilianweng.github.io/posts/2018-04-08-policy-gradient/>.
- [33] P. Wu, A. Escontrela, D. Hafner, P. Abbeel, and K. Goldberg. Daydreamer: World models for physical robot learning. In *Conference on robot learning*, pages 2226–2240. PMLR, 2023.
- [34] K. J. Young, A. Ramesh, L. Kirsch, and J. Schmidhuber. The benefits of model-based generalization in reinforcement learning. In *International Conference on Machine Learning*, pages 40254–40276. PMLR, 2023.
- [35] C. Yu, A. Velu, E. Vinitzky, J. Gao, Y. Wang, A. Bayen, and Y. Wu. The surprising effectiveness of ppo in cooperative multi-agent games. *Advances in Neural Information Processing Systems*, 35:24611–24624, 2022.

- [36] C. Yu, J. Gao, W. Liu, B. Xu, H. Tang, J. Yang, Y. Wang, and Y. Wu. Learning zero-shot cooperation with humans, assuming humans are biased. In *The Eleventh International Conference on Learning Representations*, 2023.
- [37] R. Zhao, J. Song, Y. Yuan, H. Hu, Y. Gao, Y. Wu, Z. Sun, and W. Yang. Maximum entropy population-based training for zero-shot human-ai coordination. In *Proceedings of the AAAI Conference on Artificial Intelligence*, volume 37, pages 6145–6153, 2023.

A Proof of Proposition 3.2

Proof. We assume that dynamics function F can accurately model the transition function $F(s, \mathbf{a}) \approx T(s, \mathbf{a})$ and reward function $F(s, \mathbf{a}, s') \approx R(s, \mathbf{a}, s')$ of the Dec-MDP.

For a policy pair, (π_j, π_k) A MP trajectory consists of a XP trajectory generated from XP joint policy $\pi = (\pi_j, \pi_k)$ starting from starting state $s_0 \sim p(s_0)$ and switching to a SP joint policy $\pi = (\pi_j, \pi_j)$ at timestep h . At $t = h - 1$, the state, s_{h-1} reached by XP joint policy is within $\mathcal{S}_{XP}^{j,k}$. Every subsequent state, $s_{t \geq h}$ is within the set reachable SP states from $\mathcal{S}_{SP}^j(s_{xp})$, $s_{xp} \in \mathcal{S}_{XP}^{j,k}$.

For simulated SP trajectories $\hat{\tau}_F^{\pi_{SP}}(s_{xp})$, the starting states are sampled from reachable XP states $s_{xp} \in \mathcal{S}_{XP}^{j,k}$. The subsequent simulated states are generated via SP joint policy $\pi = (\pi_j, \pi_j)$ and dynamics model F , which accurately models the true environment dynamics. Hence, every simulated state $\hat{s}_{sp} \in \hat{\tau}_F^{\pi_{SP}}(s_{xp})$ is also within the set of reachable SP states from starting state s_{xp} .

□

B Algorithm details for XPM-WM

We present the full algorithm for training an agent using XPM-WM in Algorithm 1. For the first agent, the training objective is solely the SP objective without sampling any XP trajectories.

Algorithm 1 XPM-WM Training for m -th Agent

Input: Set of $(m - 1)$ agent partners $\mathcal{D}_{m-1} = \{\pi_1, \dots, \pi_{m-1}\}$, trained World Model, \mathcal{W}_θ

- 1: Initialize actor $\pi_m^{\phi_m}$ and critics $\{v_{\psi_1}^m, \dots, v_{\psi_{m-1}}^m, v_{\psi_m}^m\}$ for agent m
- 2: Initialize self-play and cross-play replay buffer, \mathcal{B}_{SP} and \mathcal{B}_{XP}
- 3: Populate \mathcal{B}_{SP} and \mathcal{B}_{XP} with K random episodes
- 4: **while** not converged **do**
- 5: **for** $c = 0$ **to** C training steps **do**
- 6: Sample self-play and cross-play trajectories, τ_{SP} and τ_{XP} from \mathcal{B}_{SP} and \mathcal{B}_{XP}
- 7: Fine-tune World Model parameters, θ with τ_{SP} and τ_{XP} using Loss Function in (7)
- 8: Simulate joint self-play trajectories, $\hat{\tau}_W^{SP}$ from states sampled from \mathcal{B}_{SP} and \mathcal{B}_{XP} with π_{SP}
- 9: Determine current best cross-play partner $\pi_{XP} = \max_{\pi_k \in \mathcal{D}_{m-1}} J_{XP}(\pi_m, \pi_k)$ from trajectories in \mathcal{B}_{XP}
- 10: Simulate joint cross-play trajectories, $\hat{\tau}_W^{XP}$ from states in \mathcal{B}_{XP} with π_{XP}
- 11: Estimate self-play returns and compute self-play objective with $\hat{\tau}_W^{SP}$
- 12: Estimate cross-play returns and compute cross-play objective with $\hat{\tau}_W^{SP}$
- 13: Compute XPM-Sim as in (3)
- 14: Update actor parameters ϕ_m
- 15: Update critic parameters ψ_1, \dots, ψ_m
- 16: **end for**
- 17: Collect self-play episodes from environment with π_m and \mathcal{W}_θ .
- 18: Add self-play episodes to \mathcal{B}_{SP}
- 19: Sample random cross-play partner from $\pi_k \sim \mathcal{D}_{m-1}$
- 20: Collect cross-play episodes from environment with \mathcal{W}_θ , π_m and, π_k .
- 21: Add cross-play episodes to \mathcal{B}_{XP} .
- 22: **end while**

Output: m -th agent, π_m , fine-tuned World Model, \mathcal{W}_{θ^m}

C Environment description

C.1 Multi Particle Point Mass Rendezvous [4]

In this environment, two players control separate particles that can move up, down, left, right or stay in place. Four landmarks are spaces evenly in the movable space. The goal for both players is to

rendezvous at one of the four landmarks and stay there. The four landmarks represent four distinct conventions that agents pairs can converge to. Players are free to move around in the 3 by 3 unit space but the episode terminates when any player moves out-of bounds. A visualization for the initial positions of the players and landmarks can be seen in Figure 5. The Joint Rewards at each timestep is computed by the following expression:

$$JointReward = 1 - dist(\text{nearest landmark, centroid of players pos.}) - dist(\text{pos. of player1, pos. of player 2}) \quad (8)$$

where $dist(.,.)$ is the 2D Euclidean distance between two points. For the toy experiment in Section 3.1 we deterministically compute the forward dynamics of the environment using the linear dynamics provided in Multi-Particle Environment source code¹ using three scalar parameters $\{timestep, damping, sensitivity\}$.

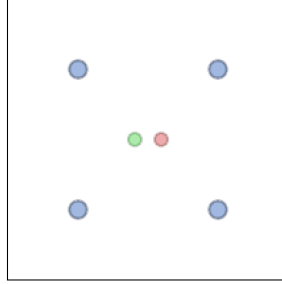


Figure 5: The initial state of Multi Particle Point Mass Rendezvous Environment. The 2 players control the red and green particles respectively. The four blue landmarks are spaced evenly in the environment. Both players receive a high reward if both particles are near one-another and to one of the landmarks. The environment episode terminates if one of the players go out of bounds of the 3x3 space.

C.2 Overcooked AI [3]

In this environment, players each control two chefs in a kitchen layout. The task is deliver as many onion soups to the counter tile in 400 time steps. The action space for each player is move left, right, up or down, no-op or to interact with an object or tile in front of them. To serve a dish of soup, players have to deposit 3 onions in the pot, wait for the pot to finish cooking and use a bowl to collect the soup before delivering it to the serving tile. We conduct our experiments on the 5 standard layouts visualized in Figure 6.

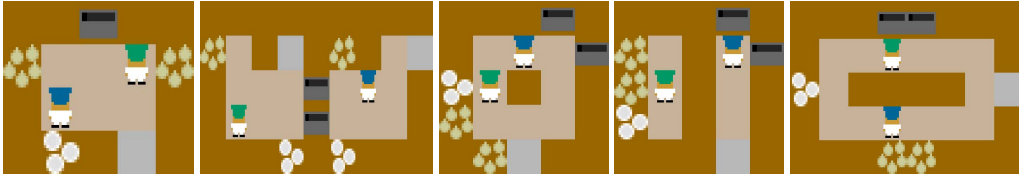


Figure 6: **The Five Overcooked layouts** From left to right: Cramped Room, Asymmetric Advantages, Coordination Ring, Forced Coordination and Counter Circuit. The Blue and Green hat chefs indicate the 2 different starting positions for each layout.

D Implementation Details

D.1 Training Algorithms

For the XPM-Sim agents in Section 3.1, we train the agents using the REINFORCE algorithm with accentralized critic and Generalized Advantage Estimation (GAE) [25] for advantage estimation.

¹<https://github.com/Farama-Foundation/PettingZoo>

For the XPM-WM Agents in Section 5, We adopt the Dreamer objective and train agents using REINFORCE with the recursive λ -target [8] for target returns estimation. For all LIPO and CoMeDI, we train all agents using MAPPO [35] with GAE.

D.2 Vectorized Reward Prediction

As described in Section 4.1, the XPM-WM reward predictor outputs a binary vector reward based on events which are then scaled by constant value. Here we describe the specific events for Overcooked AI environment and the scaling factor for each event. Note that events are player specific but the final joint reward is identical for both players.

Table 4: Reward Events for the Overcooked AI environment

Event	Reward scaling
Player i picks up ingredient	1
Player i picks up a serving bowl	1
Player i puts ingredient in pot	1
Player i picks up soup from pot	3
Player i delivers soup	12

D.3 Hyperparameters

Table 5: Hyperparameters for MPPMR Agents

hyperparameter	value
No. Actor MLP Layers	5
No. Critic MLP Layers	5
MLP Layer Size	512
activation	LeakyRELU
LIPO λ_{XP}	0.25
CoMeDi λ_{XP}	0.5
CoMeDi λ_{MP}	0.25
XPM-Sim λ_{XP}	0.5
SP, XP and MP Training steps	8e5
Simulation Horizon (XPM-Sim)	30
learning rate	5e-4
Buffer size (XPM-Sim only)	2e5
entropy coef.	1e-4

Table 6: Hyperparameters for Overcooked AI Agents (LIPO and CoMeDi) Agents. Training Steps, learning rate and Entropy coefficients are listed in order of layouts as in Figure 6.

hyperparameter	value
CNN Layers	3
CNN filter size	5x5, 3x3, 3x3
MLP Layers	2
No. Actor MLP Layers	1
No. Critic MLP Layers	1
MLP Layer Size	512
activation	LeakyRELU
LIPO λ_{XP}	0.25
CoMeDi λ_{XP}	0.5
CoMeDi λ_{MP}	0.25
SP, XP and MP Training steps (per partner)	6e6, 6e6, 6e6, 6e6, 6e6, 8e6
learning rate	6e-4, 1e-3, 8e-4, 6e-4, 6e-4
entropy coef.	3e-3, 4e-3, 5e-3, 8e-3, 8e-3

Table 7: Hyperparameters for XPM-WM on Overcooked AI Layout. Training steps are listed in order of layouts as in Figure 6.

hyperparameter	value
World Model Specific Parameters	
Encoder	3 x CNN, 3 x MLP
Decoder	3 x MLP, 3 x Transpose CNN
Transition Predictor	1 x GRU
Reward Predictor	5 x MLP
Continue Predictor	5 x MLP
Prior	2 x MLP
Posterior	2 x MLP
CNN filter size	5x5, 3x3, 3x3
GRU & MLP Layer Size	512
Joint latent dimensions	28
Agent specific latent dimensions	4
Latent classes	32
Update interval	50
WM Learning rate	2e-4
Agent Specific Parameters	
Buffer Size	1e6
Simulation Horizon	15
No. Actor MLP Layers	5
No. Critic MLP Layers	5
MLP Layer Size	512
activation	LeakyRELU
Phase 1 Training steps	2e7, 6e7, 6e7, 5e7, 8e7
Phase 2 Total Training steps per agent (SP+XP)	2e6, 2e6, 3e6, 4e6, 4e6
XPM-Sim λ_{XP}	0.25 (Other layouts), 0.1 (Counter Circuit)
actor learning rate	4e-5
critic learning rate	1e-4
entropy coef.	0.03

Table 8: Hyperparameters for XPM-WM on HiPT Ego Agent.

hyperparameter	value
CNN Layers	3
CNN filter size	5x5, 3x3, 3x3
MLP Layers	2
LSTM Layers	1
No. Actor MLP Layers	1
No. High Level Actor MLP Layers	1
No. Critic MLP Layers	1
LSTM & MLP Layer Size	512
activation	LeakyRELU
Training steps	1e8
learning rate	1e-3
entropy coef.	0.01

E Additional User Study Details

The human-AI interaction portion of this research was approved by our IRB.

All the human partners were recruited from our local university population (N=40, Woman=20, Man=20, Median Age Range=18-25 years old) via an email invitation to our in-person user study and reimbursed monetary compensation for approximately 30 minutes of their time. We did not impose any conditions on participation. We titled the study “A Study on Human-AI Collaboration” with the following description:

"Hello! In this task, you will be playing a cooking game. You will play one of two chefs in a restaurant that serves various soups. Important Guidelines for Participation and Reimbursement Eligibility

Please adhere to the following requirements to ensure your eligibility for reimbursement:

1. Game Participation

Complete all 23 games including the tutorials.

2. Active Engagement

Maintain active participation with the AI agent throughout each game by moving and interacting continuously, and trying to collaborate with AI agent. Note that inactivity exceeding 15 seconds in any game / Consistent zero rewards in the game rounds due to inactivity from your side will make you ineligible for reimbursement.

3. Player Identification

Upon completion of all game rounds, you will be assigned a unique in-game Player ID. Accurately copy and submit this Player ID in the provided Microsoft Form to ensure proper credit for your participation. Please be aware that submission of incorrect or falsified IDs will lead to disqualification.

Important Note:

Refreshing or exiting the page will reset your playing record and generate a new in-game Player ID. To maintain continuity and ensure proper credit, please complete the entire game in one session.

Movement and interactions:

You can move up, down, left, and right using the arrow keys, and interact with objects using the spacebar.

You can interact with objects by facing them and pressing spacebar. Here are some examples:

You can pick up ingredients (onions or tomatoes) by facing the ingredient area and pressing spacebar. If you are holding an ingredient, are facing an empty counter, and press spacebar, you put the ingredient on the counter. If you are holding an ingredient, are facing a pot that is not full, and press

spacebar, you will put the ingredient in the pot. If you are facing a pot that is non-empty, are currently holding nothing, and and press spacebar, you will begin cooking a soup.

Note that as you and your partner are moving around the kitchen you cannot occupy the same location.

For smooth agent movement: Press and release movement keys with brief pauses. Rapidly pressing keys continuously may cause the agent to become unresponsive.

Cooking:

Once an ingredient is in the pot, you can begin cooking a soup by pressing spacebar as noted above. You can place up to 3 ingredients in a pot before cooking.

When a soup begins cooking, you'll notice a red number appear over the pot to denote the cook time. This number counts upward until the soup is done. Soup will only be cooked when 3 onions are placed in the Pots and it will take 20 unit of time to finish cooking.

Serving:

Once the soup is in a bowl, you can serve it by bringing it to a grey serving counter.

Soups:

There are 9 possible soup recipes that can be created from combinations of tomatoes and onions, each with its own icon.

All Orders:

You can only cooked a soup with 3 onions. And this is the only order you can serve for all of the games. The All Orders list shows which recipes will receive points.

Score:

When a soup is served at the serving counter, points could potentially be added to your score.

Goal:

Your goal in this task is to serve as many of the orders as you can before each level ends. The current all orders, time, and score are all displayed in an info panel below the layout.

End of Instruction (Press "Create Game" to Start):

Now, you may click create game to start your first 3 Tutorial Games, afterward the actual rounds will be playable. You must complete 10 Recorded Rounds and submit your exit survey to receive the full credits. Please note that each game session will timeout and reset after 15 seconds of inactivity."

Upon starting the study, each participant first reads the game instruction and plays 3 tutorial games with an independent AI partner outside of the comparison baselines. Each episode lasts $T = 400$ steps (one minute). Then, each participant would play the 10 pairs of games where the layout is kept the same but the AI partners will be different. After completing all the games, the participants are requested to complete a demographic survey to indicate their gender, age group, and to provide a self-evaluation of their experience with video games as an estimation of the participant's skill level.

F Qualitative Results for MPPMR

Here we show qualitative results for the MPPMR Toy experiment. We plot the trajectories of two agents in \mathcal{D} in the MPPMR environment during cross-play from all three XPM methods. We show the agents trained under LIPO learns to go out-of-bounds while agents trained with CoMeDi and XPM-Sim stay within bounds and converge to separate landmarks.

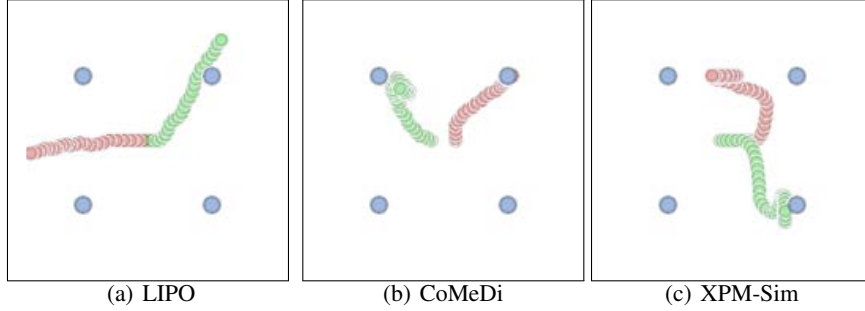


Figure 7: Trajectories of 2 sample agents under cross-play in the MPPMR environment.

G Ablation Studies

In this section we conduct additional ablation studies on different component of our proposed XPM-WM method. Specifically we show the effects of using vectorized reward prediction in the World Model. We then show the effects of using World Models on agent training, specifically the effects of the World Model as forward dynamics model of the environment. Finally we compare the wall clock time for XPM-WM as compared to other baseline methods

G.1 Effect of Vectorized Reward Prediction

Here we test the effect of using vectorized reward prediction when training the World Model. We include a variant of XPM-WM that predicts only a scalar joint reward at the reward predictor (modeled as Gaussian distribution) and compare with XPM-WM with vectorized rewards. We plot the training curves for Phase 1 of the training process in Figure 8. Our results show without explicitly factoring rewards, the world model fails to learn any meaningful policies.

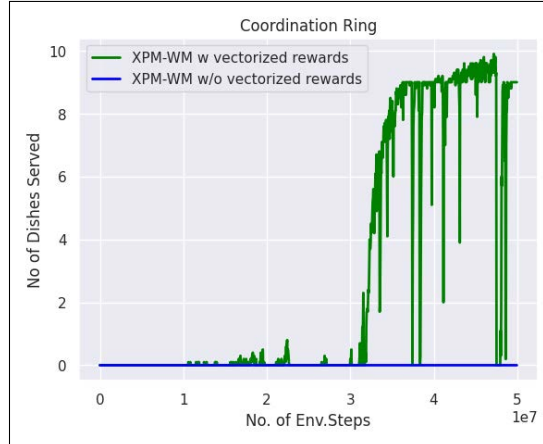


Figure 8: A comparison of the training curves for XPM-WM with and without the use to vectorized event-based reward prediction on the Coordination Ring layout.

G.2 Effect of World Model as a Dynamics Model

In this section we investigate the role of the World Model as a dynamics model on training efficiency. To do that we would need to decouple the dynamics modeling effects of the World Model from its role as a shared encoder for learning compact representations of the joint state. Hence we revisit MPPMR environment for this study. Specifically, we train a shared encoder network that is shared across all agents in the population while simulated trajectories can still be generated by the deterministic dynamics model that are separate from the agents. For the shared encoder, we

first train the initial agent together with a Variational Autoencoder (VAE) [13]. The VAE is trained to reconstruct the joint observation. The actor and critic takes in the latent representation of the VAE. The shared encoder is then used to bootstrap training for subsequent agents and VAE is still continuously updated similar to XPM-WM.

We compare the training efficiency of this agent population to the one we describe in Section 3.1 (separate agents without the shared encoder). We plot the average learning curves across all 8 agents in Figure 9. Our results show that agents trained with the shared encoder actually has a performance compared to agents trained without a shared encoder. We hypothesize is that this might be due to the fact that the shared encoder might have over-fitted to the state distribution of a particular (set of) partners and are therefore ill-suited as encoder for other partners which encounters states that are out of distribution for the encoder and it requires additional finetuning steps to re-align the encoder to the distributional shift, whereas a world model that is train to model the forward dynamics of the environment can still meaningfully represent states that are out of distribution.

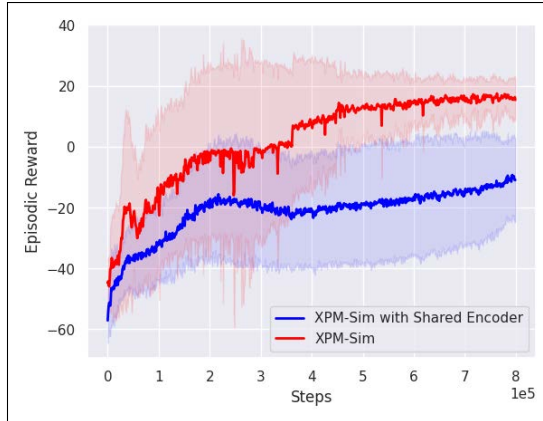


Figure 9: A comparison of the training curves for agents 2-8 for XPM-Sim with and without the shared encoder on the MPPMR environment. For XPM-Sim with shared encoder, we first train the first agent together with a VAE. The VAE is trained to reconstruct the joint observation. The actor and critic takes in the latent representation of the VAE. The shared encoder is then used to bootstrap training for subsequent agents and VAE is still continuously updated similar to XPM-WM.

G.3 Training Wall Clock Time

In this section we compare the wall clock training time of XPM-WM as compared to CoMeDi and LIPO. We train all 8 agents on a single NVIDIA 4090 GPU and plot the cumulative wall clock time of training each subsequent agent. In Figure 10 we plot the wall clock time agents 1 to 8 which includes the World Model training for the initial agent. In Figure 11 we plot wall clock time for agents 2 to 8. We show that similar although training the World Model requires significantly more time compared to other baselines, subsequent agents actually are more time efficient as time cost for XPM-WM agents increase at a linear rate while agents trained using CoMeDi and LIPO increase at a steeper non-linear rate, suggesting the XPM-WM will overall also be more time efficient as we scale up the number of agents.

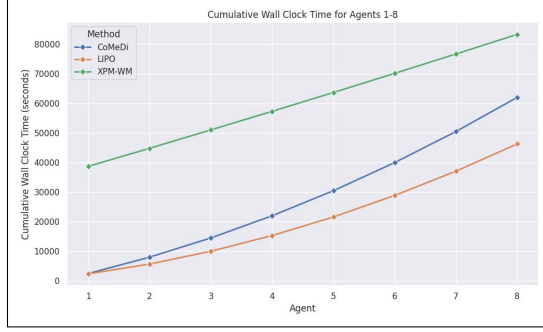


Figure 10: A comparison of the training wall clock time for XPM-WM with CoMeDi and LIPO for all 8 agents on the Coordination Ring layout.

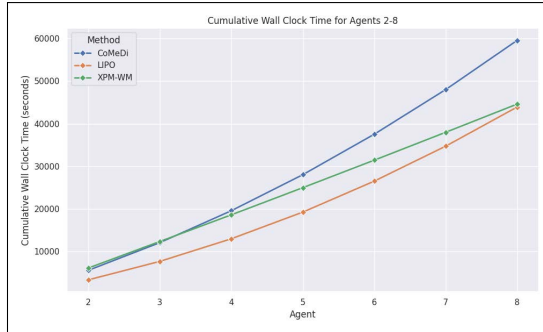


Figure 11: A comparison of the training wall clock time for XPM-WM with CoMeDi and LIPO for agents 2-8 (Phase 2 training only) on the Coordination Ring layout.

H Additional Results For Overcooked AI

In this section we show the SP training curves of XPM-WM as compared to other baseline methods. We plot the training curves of each subsequent agent, i.e. agents $m=2$ to $m=8$. Our results, which we show in Figure shows the increase in sample efficiency and performance of an agent that is bootstrapped by a pre-trained World Model versus a agent that is trained from scratch.

H.1 Training Curves

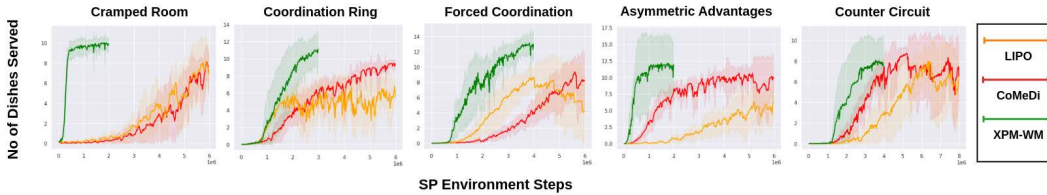


Figure 12: Training Curves for all 5 Overcooked layouts. We plot the number of dishes served in each environment in each layout against the number of **SP training steps** (steps from XP and MP trajectories are excluded) averages across each subsequent agent in the population. The bold lines are the average dishes served across all subsequent agents and shaded area indicate the standard deviation.

H.2 Average SP and XP Results.

In this section we show the average SP and XP scores of the agents generated using XPM-WM and compare them with the other XPM baselines. XP scores are averaged over every other agent in the population at both starting positions.

Table 9: The average number of dishes served in Self Play and Cross Play across all 5 Overcooked Environments for each method of XPM-based diverse agent population generation. Both self play and cross play scores are averaged over 20 episode of 400 steps

Layout	LIPO		CoMeDi		XPM-WM (Ours)	
	SP \uparrow	XP \downarrow	SP \uparrow	XP \downarrow	SP \uparrow	XP \downarrow
Cramped Room	8.99	2.40	8.29	1.58	10.23	0.43
Asymmetric Advantages	9.07	1.76	11.23	6.80	18.28	0.83
Coordination Ring	7.77	0.11	9.45	2.74	10.81	0.03
Forced Coordination	10.50	1.99	8.84	1.61	14.23	0.07
Counter Circuit	8.47	0.36	8.94	1.26	8.25	0.72
Average	8.95	1.32	9.35	2.80	12.36	0.42

H.3 Ego Agent Results for Specific Overcooked Layouts

Table 10: Cramped Room

	E-LIPO	E-CoMeDi	E-XPM-WM
LIPO	7.04 ± 3.25	6.75 ± 3.14	5.36 ± 3.14
CoMeDi	7.96 ± 3.19	7.43 ± 3.44	7.44 ± 2.89
XPM-WM	7.04 ± 3.55	7.34 ± 3.07	8.75 ± 2.13
Average	7.35 ± 3.33	7.17 ± 3.22	7.18 ± 2.75

Table 11: Asymmetric Advantages

	E-LIPO	E-CoMeDi	E-XPM-WM
LIPO	13.07 ± 4.42	7.75 ± 5.23	7.61 ± 5.05
CoMeDi	12.82 ± 3.94	10.09 ± 6.05	10.00 ± 4.65
XPM-WM	10.21 ± 6.29	4.68 ± 5.81	10.33 ± 6.71
Average	12.03 ± 4.99	7.51 ± 5.71	9.31 ± 5.54

Table 12: Coordination Ring

	E-LIPO	E-CoMeDi	E-XPM-WM
LIPO	3.52 ± 2.17	2.44 ± 2.69	2.64 ± 1.90
CoMeDi	4.65 ± 2.38	3.52 ± 2.81	3.80 ± 2.18
XPM-WM	3.13 ± 1.98	0.81 ± 1.99	3.85 ± 3.58
Average	3.77 ± 2.18	2.26 ± 2.52	3.43 ± 2.24

Table 13: Forced Coordination

	E-LIPO	E-CoMeDi	E-XPM-WM
LIPO	3.38 ± 3.70	7.12 ± 3.17	3.95 ± 2.76
CoMeDi	1.27 ± 2.16	5.70 ± 2.92	4.47 ± 2.85
XPM-WM	1.53 ± 1.88	3.54 ± 3.22	4.91 ± 3.69
Average	2.06 ± 2.70	5.45 ± 3.11	4.44 ± 3.13

Table 14: Counter Circuit

	E-LIPO	E-CoMeDi	E-XPM-WM
LIPO	2.30 ± 2.21	2.55 ± 2.80	3.21 ± 2.93
CoMeDi	4.47 ± 3.11	3.29 ± 2.90	6.07 ± 2.35
XPM-WM	1.48 ± 2.41	1.15 ± 2.43	4.70 ± 2.35
Average	2.75 ± 2.61	2.33 ± 2.72	4.66 ± 2.56

I Related Work

World Models: World Models have been a popular branch of Model-Based Reinforcement Learning methods, most prominent of which are the Dreamer models [7–9], which learn the state transitions in form of a Recurrent State Space Model (RSSM) and allow agents to learn via simulated trajectories. World Models have been applied to many areas of intelligent control such as simulating entire game environments using large scale training data [2, 28], and in real-world situations such as robot control and navigation [33, 1] and autonomous driving [31, 10]. In the multi-agent context, Venugopal et al. [29] proposed MABL, which adapts the Dreamer model for a Multi-Agent Reinforcement Learning setting, in which agents in a team are trained jointly. MABL divide the world model into a hierarchical model consisting global and agent specific level. Our method does not explicitly separate the global and agent level representations at the architecture level but instead split the latent representations itself into global and agent-specific representations.

Another related work using WM is by Prasanna et al. [21], which proposed using world models for Zero-Shot Generalization of single-agent RL agents. They propose doing so by adding contextual information into world model to allow agents to generalize to out-of distribution tasks. Though we are also interested in the generalization to unseen partners in zero-shot, we instead employ world models as a means to efficiently generate new partner agents to train a robust ego agent that can do Zero shot Coordination.

Other Methods for DiversePopulation Generation: TrajeDi [20] and MEP [37] uses Jensen-Shannon Divergence objective on policy trajectories and states of each partner agent to train a statistically diverse set of partner agents. FCP [27] does not impose any additional training objectives but instead include past checkpoints of fully trained agents to simulate less skillful agents. Finally, HSP [36] trains individual agent with hidden biased reward on top of the existing environmental rewards. The hidden rewards are randomly sampled for each agent based on sub-events within the environment. A best-response policy is then trained together with each biased agent and the biased-best response agent pair is then added to form the pool of partner agents.

Similar to our method, ADVERSITY [5] also utilize model-based methods for cross-play minimization, specifically to learn a incompatible policy from a repulser policy in a partially observable environment of Hanabi. Rather than learning a world model, ADVERSITY instead learns a belief model [12], which models behavior of the partner agents as well the true trajectory/state. ADVERSITY then uses the belief model to generate fictitious transitions similar to how World Model generates simulated trajectories. ADVERSITY also requires training multiple belief models for agent which is expensive to compute as the number of agents increases. Our method instead only learns one World Model that gets continuously gets fine-tuned over the training process of every agent.

J Limitations

Though XPM-WM presents a more sample efficient method for generating diverse cooperative partners, there are some key limitations to the current method. A primary limitation is that due to the fact XPM-WM requires learning an accurate World Model of the environment, it is unclear how it would handle cases where agents have partial observability of the true state. This can potentially be mitigated if the true global state is available but this information might not be readily available for all tasks.

Another limitation is that it also unclear how our method scales to more multi-agent tasks of more than 2 players as sampling cross-play trajectories might become exponentially more complex as the number of players in the environment increases. We plan to meaningfully address both these limitations in our future work.

K Broader Impact

We believe our proposed method XPM-WM can potentially bring positive impact in the field of Human-AI Collaboration by enabling much more efficient generation of diverse partners. However, as our method is used to train agents that directly interact with humans, we recognize that a more advanced version of our methods (such as those powered with Foundation Models) can potentially be used to coerce humans and negatively influence the behaviors of humans. We also like to emphasize that the current version of our method is only used for small game-like environments and is we believe unlikely to cause any negative influence on humans that will result in significant long-term societal harm.

L Creative Assets

This work uses assets from the Overcooked AI environment [3] which is open-sourced under the MIT license.